The Conformation of Dolichol†

Nicholas J. Murgolo, Akhileswar Patel, Salvatore S. Stivala, and Tommy K. Wong*
Department of Chemistry and Chemical Engineering, Stevens Institute of Technology, Hoboken, New Jersey 07030
Received January 20, 1988; Revised Manuscript Received August 17, 1988

ABSTRACT: An understanding of the natural conformation of dolichol is important for the elucidation of the mechanism of protein glycosylation and dolichol's other as yet undisclosed biological functions. Since the molecular mechanics method has been shown to be well suited for the prediction of alcohol and alkene conformations, we have employed it to study the conformations of apparent least energy of dolichol-19 and smaller polymers of isoprene, namely, squalene, *trans,trans*-farnesol, and *cis,cis*-farnesol. Additionally, the small-angle X-ray scattering (SAXS) method was employed to determine the validity of the apparent least energy conformer of dolichol-19 derived by the molecular mechanics method. The results indicate that the solution conformation of dolichol-19 is comprised of a central coiled region flanked by two arms. The central coiled region has two and a half turns of dimensions 9.84 × 16.55 × 51.66 Å^3. The arms of dimensions 3.99 × 5.89 × 17.47 Å^3 and 4.49 × 9.23 × 11.14 Å^3 are approximately diametrically opposed. Measurement of the intrinsic viscosity of dolichol in both isopentyl alcohol and oleyl alcohol showed that the natural conformation of dolichol is capable of increasing solution fluidity (i.e., lowering solution viscosity). Thus, while examination of the conformation of dolichol in a membrane-mimetic solvent by SAXS is not possible, the quantitative measure of the effect of dolichol on solution viscosity (and thus solution fluidity) is possible. The results are consistent with dolichol acting as a membrane-fluidizing agent and provide the first quantitative measure of the effect of dolichol on solution fluidity of a membrane-mimetic solvent.

Dolichol, a naturally occurring polyisoprenoid alcohol, was first discovered in mammalian tissues in the early 1960s (Burgos et al., 1963). It has been shown that dolichol is polydispersed, ranging from 16 to 21 isoprene units, depending on the species studied (Dunphy et al., 1967). In the case of dolichol from pig liver, the most predominant form is composed of 19 isoprene units. We have previously demonstrated that the relatively low polydispersity of dolichol allows analysis by small-angle X-ray scattering (SAXS) without necessitating fractionation (Murgolo et al., 1987). It is now well established that the mono- and diphosphate derivatives of dolichol participate in the N-linked glycosylation of proteins in the rough endoplasmic reticulum (Struck & Lennarz, 1980). However, the process by which sugars are translocated by dolichol derivatives in the glycosylation of proteins in the rough endoplasmic reticulum has not been delineated. Knowledge of the conformations of dolichol or its derivatives is a necessary first step toward the understanding of the functions of these isoprene derivatives.

Dolichol-19 is composed of 1 saturated α-isoprene unit of the *R* configuration, 15 intermediate isoprene units of the cis configuration, and 3 terminal *trans*-isoprene units. It has been proposed that, in its fully extended form, dolichol-19 is about 100 Å in length (Struck & Lennarz, 1980). This is in good agreement with our previously determined extended conformation of pig liver dolichol in CCl_4, a good penetrating solvent (Murgolo et al., 1987). Clearly, the natural conformation is very unlikely to be the extended form since the widths of biological membranes are generally of the order 50–70 Å. A helical structure of about 70 Å in length, approximated by a CPK model, has been proposed (Keenan et al., 1977). However, computational or chemical data supporting this model were not presented. To date, the only computational study of the conformations of dolichol was our recent presentation of the molecular mechanics determined structure of dolichol (Murgolo & Wong, 1986).

Together with the expansion of the molecular mechanics program in our laboratory, a few recent advances in the determination of conformation by the molecular mechanics method make the determination of dolichol's conformation possible. These developments are the following: the development of a more accurate MM2 force field (Allinger, 1977); the demonstration of this force field's ability to accurately predict the conformations of alkanes and nonconjugated alkenes (White & Bovill, 1977); the development of force field constants for the application of this method to alcohols (Burkert, 1979; Allinger & Chung, 1976); and the recent application of the MM2 method to the study of the conformation of the bilayer lipid docosahexaenoic acid (Applegate & Glomset, 1986). In the molecular mechanics method an educated guess is made as to the conformation of least steric energy of a test compound. The conformation is then transformed through several rotamers moving in the direction that will minimize the gradient of the steric energy to the greatest extent. The energy of each resulting geometry is determined by the application of an empirical classical model for steric energy. The calculation terminates when a minimum of the potential energy surface of the test compound is reached. Since constants for the phosphate or pyrophosphate groups for use in the molecular mechanics method have yet to be developed and since the conformation of the hydrocarbon chains of dolichols in the biological membrane is of primary interest, we have chosen here to analyze the conformation of dolichol-19. We intend to describe this conformer and to present SAXS results verifying this structure.

Materials and Methods

Energy-minimization computations were performed on Digital Equipment Corporation (DEC) VAX 11/780 and

† This research was supported by a grant from Research Corporation to T.K.W. This paper (or part thereof) has been submitted by N.J.M. in partial fulfillment of the requirements for the Ph.D. degree in the Department of Chemistry and Chemical Engineering at Stevens Institute of Technology.

0006-2960/89/0428-0253$01.50/0

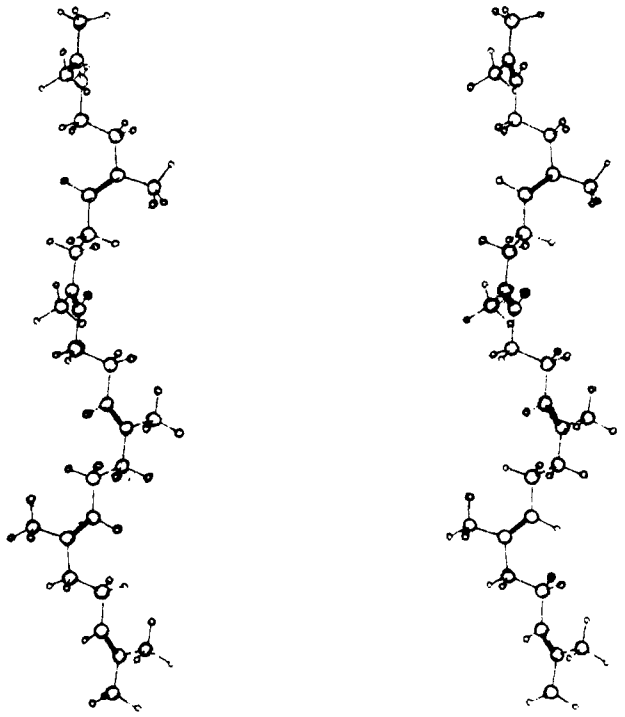

FIGURE 1: Stereoprojection of squalene.

11/785 virtual memory computers. Stereographic plots were drawn on a Houston Instruments Calcomp 1039 plotter. Graphics were assisted by the software package DI3000 manufactured by Precision Visuals, Inc.

Molecular Mechanics Method. The molecular mechanics method, the FORTRAN program MM2 (Allinger, 1977), was employed with the standard MM2 parameters. The array dimensions of this method were adjusted to a maximum of 500 atoms. This method was then applied to determine the apparent least-energy conformations of dolichol-19, squalene, *cis,cis*-farnesol, *trans,trans*-farnesol, and cholesterol. The principles behind the molecular mechanics method have been thoroughly outlined elsewhere (Wilberg, 1965; Allinger, 1977; Engler, 1973). Units of energy were invariably kilocalories per mole.

Small-Angle X-ray Scattering (SAXS). Pig liver dolichol and oleyl alcohol were obtained from Sigma (St. Louis, MO). Isopentyl alcohol was obtained from Aldrich (Milwaukee, WI). The experimental details of the SAXS experiments were similar to those outlined in our previous publication (Murgolo et al., 1987). One important difference is that a counting time of 400 s was employed in the isopentyl alcohol and oleyl alcohol studies. Since isopentyl alcohol and oleyl alcohol are not as volatile as CCl_4, longer counting times were employed. The longer counting time ensured a low statistical error. Only one sample (20 mg/mL) of dolichol in oleyl alcohol was analyzed by SAXS as it was observed that dolichol ordered this solvent. Solutions of 10, 20, 30, and 40 mg/mL dolichol in isopentyl alcohol were prepared for SAXS. Several solutions of various concentrations were prepared for the measurement of the partial specific volume and intrinsic viscosity of dolichol in isopentyl alcohol and the intrinsic viscosity of dolichol in oleyl alcohol. The technique for the calculation of SAXS parameters from scattering data and for the prediction of SAXS parameters from theoretical conformations was outlined in our previous publication (Murgolo et al., 1987).

Table I: Variation of Total Steric Energy of *cis,cis*-Farnesol with Changing Torsional Angle between Methylene Groups Adjacent to Central Double Bond

E (steric)[a]	ϕ (torsional angle)[a]	E (steric)[a]	ϕ (torsional angle)[a]
40.78	0.00	39.38	60.00
39.87	−60.00	39.32	−43.00

[a] E is the total steric energy in kcal/mol and ϕ is the torsional angle between the hydrogens immediately adjacent to the central double bond in deg.

Results

The ability of our version of the molecular mechanics program MM2 to predict molecular conformations of polyisoprenoids was demonstrated by squalene. When the crystal structure of squalene was given as a starting geometry in the energy-minimization scheme, all conformers formed by alteration of the crystal structure were found to have more steric energy than the crystal structure. When a planar form of squalene was entered into MM2 as an initial conformer, the minimization process resulted in a reversion to the crystal structure as that of the lowest energy. This result demonstrates, therefore, that the molecular mechanics method was able to predict the crystal structure of isoprenoid compounds as lowest energy conformers. The energy-minimized conformer of squalene is shown as a stereoprojection in Figure 1.

When a planar form of *trans,trans*-farnesol was entered as an initial conformational guess for energy minimization with MM2, the resulting conformation of least energy was found to have a 63° kiltering (with respect to the planar form) that was very similar to squalene's conformation. This apparent lowest energy conformer was found to be identical with a conformer generated by cutting the energy-minimized conformer of squalene in half, followed by energy minimization of the hydroxyl group. A stereoprojection of the energy-minimized form of *trans,trans*-farnesol is provided in Figure 2.

When *cis,cis*-farnesol was energy minimized, it was found that the molecule possessed a kink about the single bond on the α side of its central double bond. When a planar form of *cis,cis*-farnesol was the initial guess input, the resulting energy-minimized conformation was found to exist in a nonplanar, bent form. When the nature of this kink was examined with respect to the torsional angle between the hydrogens or the methylene groups immediately adjacent to the central double bond on either side, the position of lowest energy was determined (Table I). This interaction is responsible for the coiled nature of the central portion of dolichol-19 as is shown

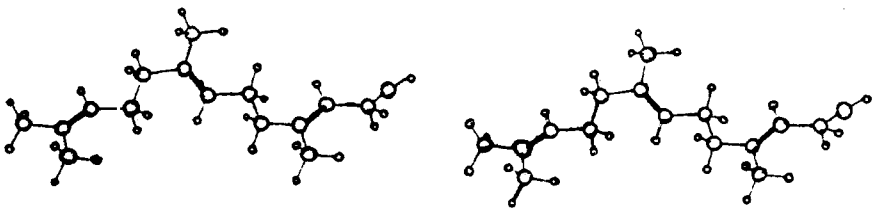

FIGURE 2: Stereoprojection of *trans,trans*-farnesol.

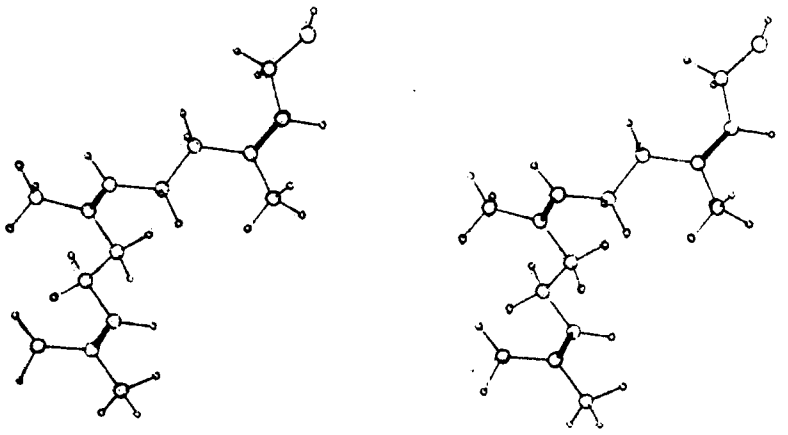

FIGURE 3: Stereoprojection of *cis,cis*-farnesol.

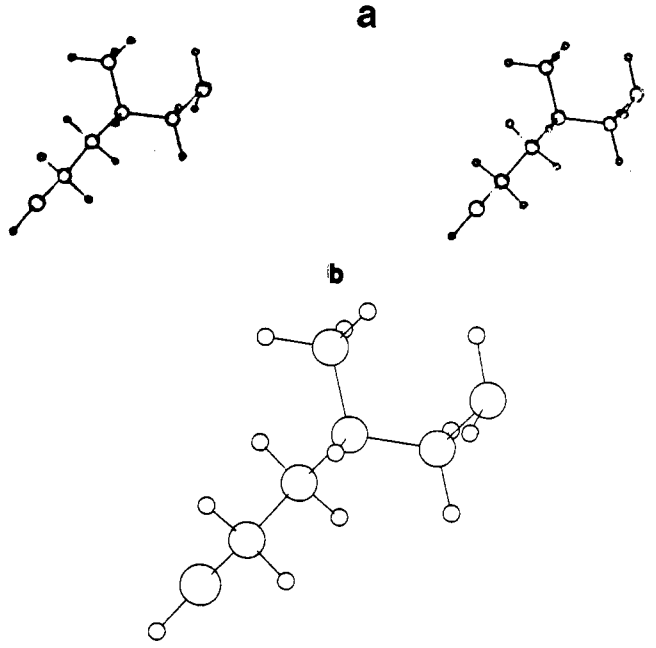

FIGURE 4: (a) Stereoprojection of section A of dolichol-19. (b) Three-dimensional plot of section A of dolichol-19.

Table II: Steric Energies of Apparent Lowest Energy Conformers of a Few Isoprenoid Species

species	*E* (steric) (kcal/mol)	species	*E* (steric) (kcal/mol)
cis,cis-farnesol	39.32	squalene	48.22
trans,trans-farnesol	34.10	dolichol-19	510.43

Table III: Geometric Parameters of the Apparent Lowest Energy Conformers of a Few Isoprenoid Compounds

species	dimensions (Å^3)
cis,cis-farnesol	6.02 × 8.95 × 11.26
trans,trans-farnesol	5.74 × 6.79 × 13.59
squalene	6.49 × 8.17 × 26.23
dolichol-19	
whole molecule	12.48 × 30.94 × 53.07
section A	3.99 × 5.89 × 17.47
section B	9.84 × 16.55 × 51.66
section C	4.49 × 9.23 × 11.14
angle between sections A and B	96.65°
angle between sections A and C	159.08°
angle between sections B and C	93.74°
average radius of section B coil	2.93 ± 0.36 Å

below. A stereographic projection of the lowest energy conformer of *cis,cis*-farnesol is given in Figure 3.

By use of the method of molecular mechanics, the lowest steric energies of dolichol-19 and each of the isoprenoids under investigation were determined and are provided in Table II. The lowest steric energy conformer of dolichol-19 was found to have three geometrical regions: a central coiled portion and two flanking arms. The portion that contains the α (saturated) isoprene is section A of the molecule; the central coiled region is section B; and the terminal arm that has the same configuration as *trans,trans*-farnesol is section C. A measure of dimensions of all of the isoprenoids studied, including the distinct regions of dolichol-19, was obtained by enclosing the molecules in rectangular boxes defined by their extrema. The dimensions of each isoprenoid molecule are provided in Table III. The angle between each section was determined by finding the direction cosines of lines characteristic of each section. It was found that the two arms were very nearly perpendicular to the central coiled section. Further, the arms did not cover the center of the central coiled region, and they were not quite oppositely directed. The stereoprojection and three-dimensional plots of section A are provided in Figure 4. For the central coiled region (section B), it was determined that the section consisted of approximately two and a half turns. When perpendicular line segments were dropped from each atom in section B to the center line (only those atoms that comprised the backbone were involved, and the hydrogens and external methyl carbons were excluded), the average radius of the coiled section was found to be 2.93 Å with a standard deviation of 0.36 Å. It was also observed that the coil is of approximately uniform diameter throughout its entire length. A stereoprojection of section B is provided in Figure 5 in which hydrogens have been removed to aid visualization of this coiled region. A stereoprojection and three-dimensional plot of section C is provided in Figure 6.

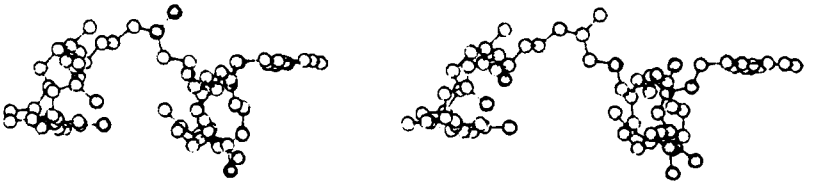

FIGURE 5: Stereoprojection of section B of dolichol-19, with hydrogens removed.

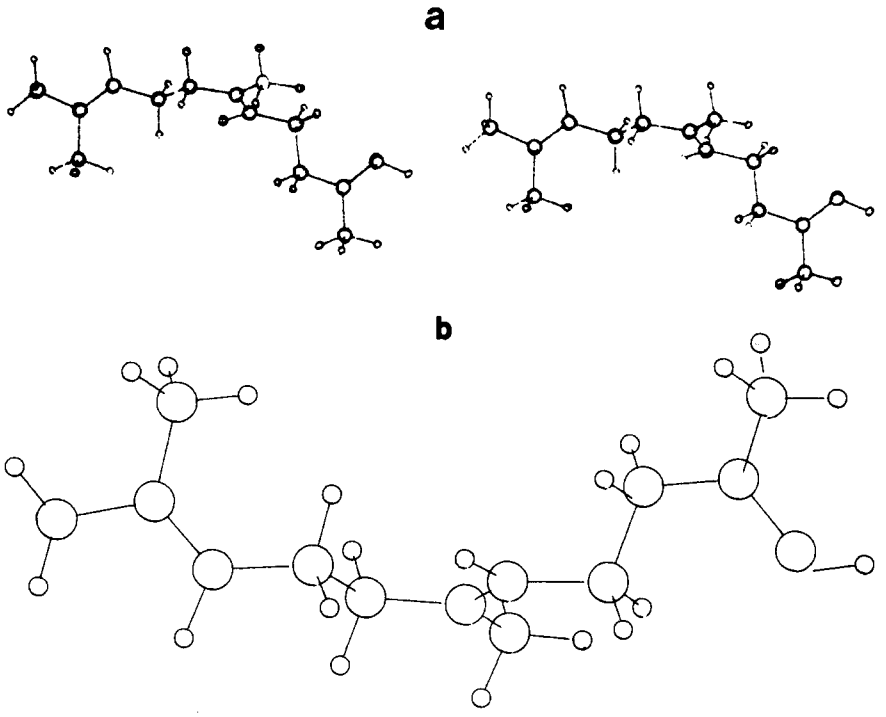

FIGURE 6: (a) Stereoprojection of section C of dolichol-19. (b) Three-dimensional plot of section C of dolichol-19.

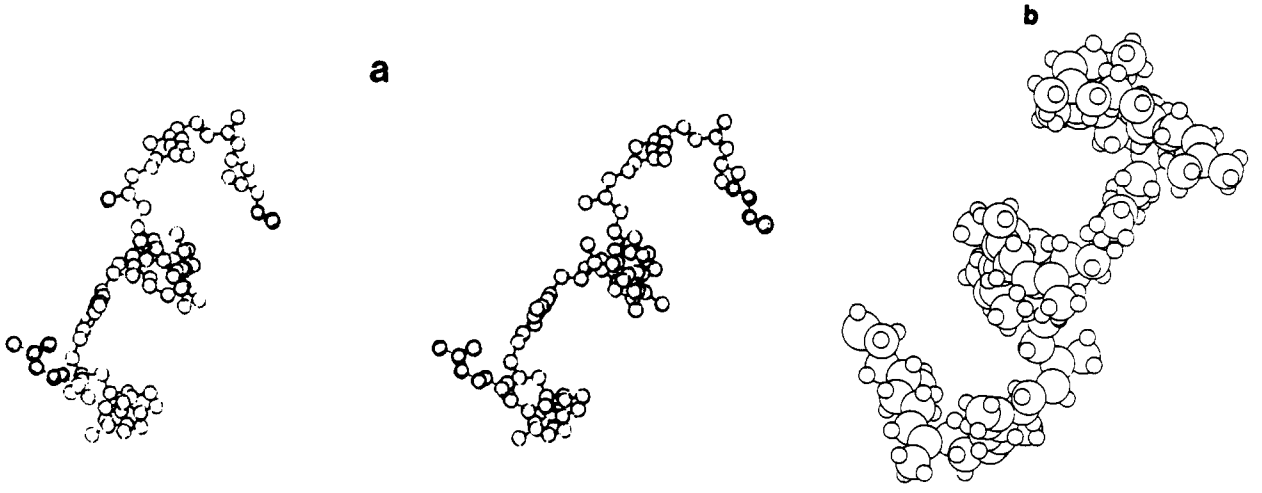

FIGURE 7: (a) Stereoprojection of dolichol-19, with hydrogens removed. (b) Three-dimensional plot of dolichol-19.

Figure 7 shows stereoprojection and three-dimensional plots of the energy-minimized conformer of dolichol-19. As with section B, hydrogens have been removed to aid visualization.

Structural parameters determined from the SAXS study of dolichol-19 in isopentyl alcohol, compared with those theoretically derived from the molecular mechanics, are presented in Table IV. The basis of the techniques employed have been previously delineated in our study of the extended conformer (Murgolo et al., 1987). A plot of the scattering intensities (smoothed and corrected from transmission) versus camera position is provided in Figure 8. The small difference between the scattering intensities of the dolichol solutions and the solvent mandated that the SAXS parameters could only be accurately predicted for the 30 and 40 mg/mL solutions, as the lower concentrations did not scatter enough to be interpreted over the basal noise level. We have also included data from our prior theoretical and SAXS study of the extended conformer of dolichol-19 in Table IV. The lower values of R_g, R_q, and a^* all indicate a more compact structure than the extended conformer for the solution conformation. The closer agreement of experimental and theoretical data for R_g is satisfactory and lends support to the methodologies. The difference between the expected and determined values of persistence length demonstrates mobility in the arms, as the calculation of the value is extremely sensitive to the relative position of sections A and C. The plot of the electron density distribution function of dolichol, derived from the isopentyl

Table IV: Comparison of the Solution Conformation and the Extended Conformation of Dolichol

	solution conformation		extended conformation[c]	
parameter[a]	SAXS[b]	theoretical	SAXS[d]	theoretical
R_g (Å)	19.87	18.98	27.70	25.21
R_q (Å)	8.17	7.84	14.73	15.11
a^* (Å)	23.74	17.93	46.00	42.82

[a] R_g is the radius of gyration, R_q is the radius of gyration of the cross section, and a^* is the persistence length. [b] Small-angle X-ray scattering studies of dolichol in isopentyl alcohol. [c] Murgolo et al. (1987). [d] Small-angle X-ray scattering studies of dolichol in CCl_4.

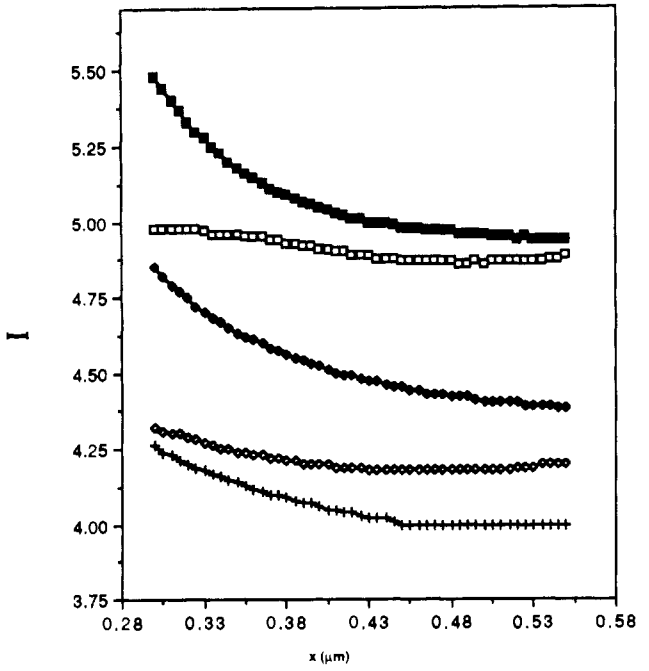

FIGURE 8: Scattering intensities of dolichol in isopentyl alcohol. The concentrations of dolichol in isopentyl alcohol are (+) 0 mg/mL, (○) 10 mg/mL, (♦) 20 mg/mL, (□) 30 mg/mL, and (■) 40 mg/mL.

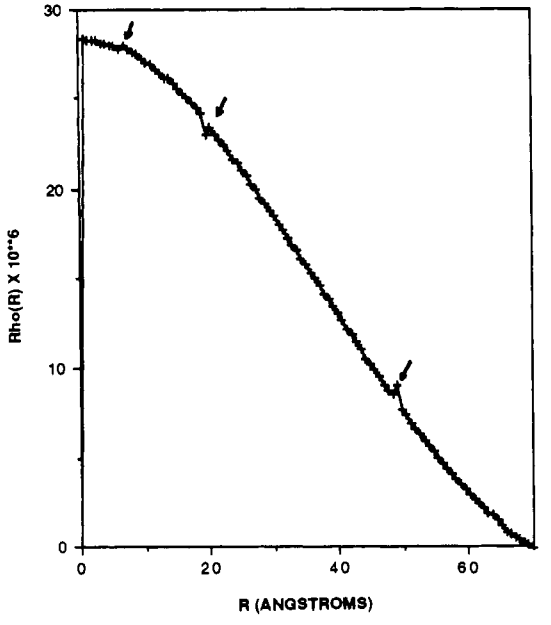

FIGURE 9: Electron distribution function of dolichol calculated on the basis of SAXS data in isopentyl alcohol.

alcohol SAXS study, gives further validity to this assertion (see Figure 9). Two of the increased values correspond to the diameter and turn-to-turn distance (pitch) of the coil; the relatively small third value is less than the separation in space of sections A and C in the energy-minimized structure. Taken together, these points suggest certain motion of sections A and C relative to each other, with the integrity of the central coiled section B being maintained. The comparison of the electron distribution functions of the dolichol-19 in isopentyl alcohol and CCl_4 is provided in Figure 10. These results coupled with the lower values of R_g, R_q, and a^* in the isopentyl alcohol study suggest that the solution conformation of dolichol is far more compact than the extended conformation. Furthermore, calculation of a theoretical distance distribution function for a spherical molecule of R_g = 19.87 Å and its comparison to the actual distance distribution function of dolichol obtained

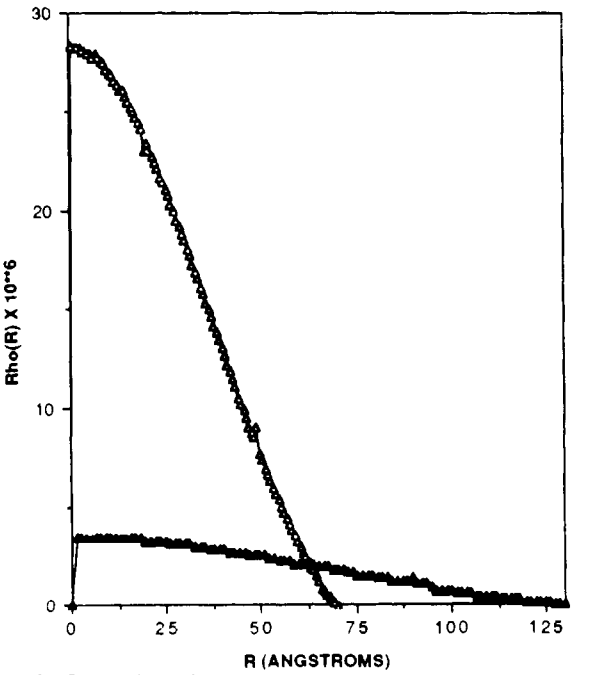

FIGURE 10: Comparison of the electron distribution function of dolichol calculated on the basis of SAXS data in isopentyl alcohol (△) and CCl_4 (▲).

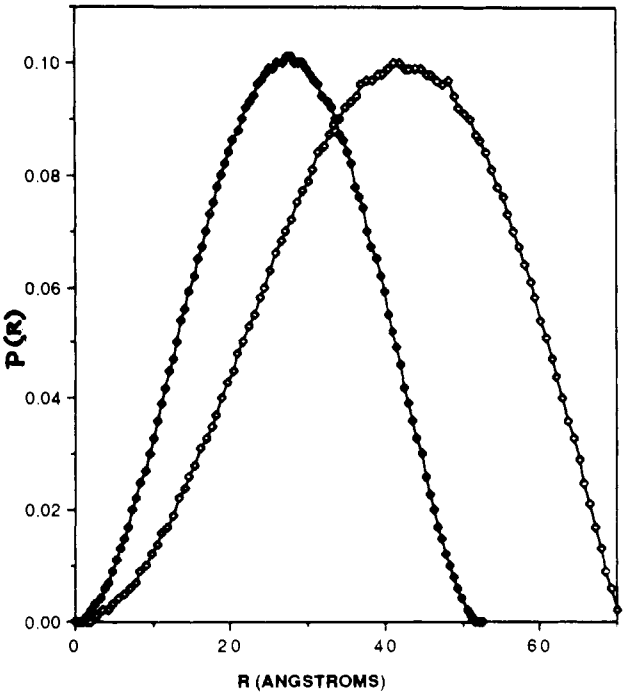

FIGURE 11: Comparison of the correlation function (density distribution function) of dolichol from isopentyl alcohol SAXS data (○) and that expected for a theoretical sphere of similar R_g (●).

from this SAXS study are given in Figure 11. The results show that alcohol dolichol does not exist in its completely extended conformation in isopentyl alcohol, it is not as compact as a spherical distribution.

The sources of errors in SAXS (Kratky, 1983) are (a) polydispersity of the sample, (b) interparticle interference, (c) the effect of beam geometry, (d) radiation damage, (e) stability in experimental environment, and (f) counts statistics. Since the polydispersity index of dolichol was 1.004 (Murgolo et al., 1987) and the scattering intensities at zero angle have been extrapolated for zero concentration, the errors due to polydispersity and interparticle interference are minimal. The error

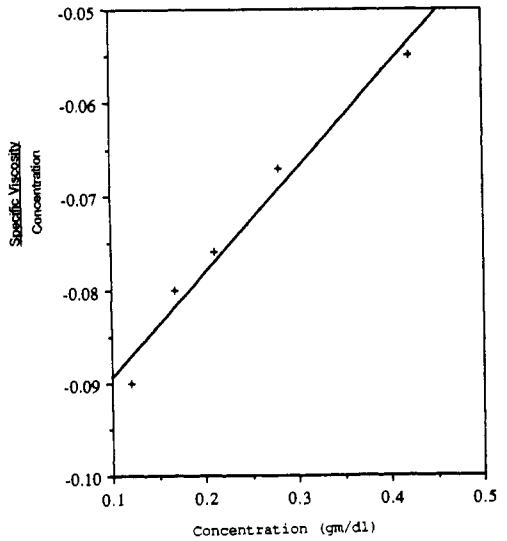

FIGURE 12: Intrinsic viscosity of dolichol in isopentyl alcohol.

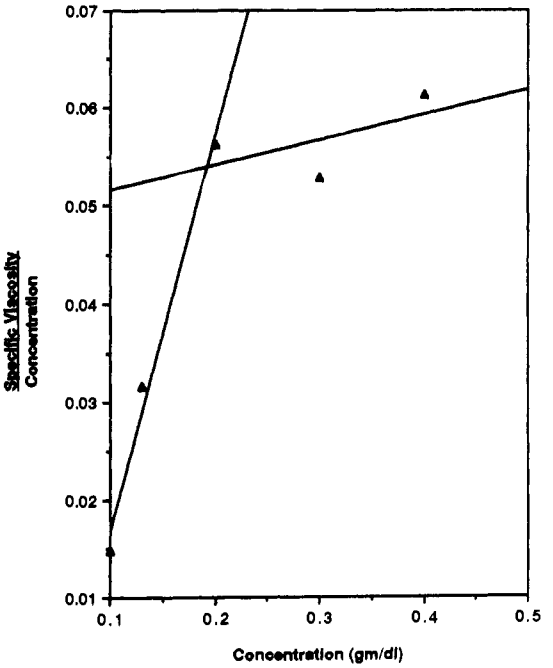

FIGURE 13: Intrinsic viscosity of dolichol in oleyl alcohol.

due to beam geometry is eliminated by desmearing the scattering intensities as per the computer program of Glatter (1977). It has been observed by Kratky (1983) that irradiation with X-rays (λ = 1.5418 Å) for days induces no measurable perturbation in most cases. Since our exposure time per sample was less than 12 h, we do not anticipate any radiation damage. Our experimental environment has been stabilized with a temperature fluctuation of ±1 °C, as recommended by Kratky (1967). The only error that might have been involved in our measurements would be the counts statistics, since we collected counts for 400 s at every angular position. However, we have smoothed this scattering curve by a computer program to minimize the data fluctuation. Our recent work (unpublished) on a standard polystyrene (M_w = 4630, Polyscience) gave an error of 0.2% in the molecular weight measurement from SAXS.

The plots of reduced viscosities versus concentrations of dolichol-19 in isopentyl alcohol and oleyl alcohol are shown in Figures 12 and 13, respectively. The nature of the plot in Figure 13 suggests a micellar aggregation of oleyl alcohol above 0.2 gm/dL. The profiles of dolichol in both oleyl alcohol and isopentyl alcohol are suggestive of the fact that dolichol plays the role of solution fluidizer.

Discussion

We chose to analyze the conformation of dolichol-19 as a representative conformation of the entire class of dolichol molecules, including phosphate derivatives. The difficulties encountered in the generation of phosphate data for the molecular mechanics program MM2 have been recently presented (Burkert & Allinger, 1982). Although a force field has been developed for molecular dynamics calculations of protein and nucleic acid conformations (Weiner et al., 1984), its phosphate constants are not compatible with our current MM2 field. While the molecular dynamics method has been shown to accurately predict conformational dynamics of proteins, we feel that the higher inaccuracy of the molecular dynamics force field as compared with the molecular mechanics force field would make the prediction of conformations of relatively flexible polyisoprenoids inaccurate. In addition, molecular dynamics force fields have been developed for the determination of protein conformation and may not perform well in the prediction of conformations of polyisoprenoids.

The close agreement of the integrity of the coiled region as determined from the correlation of the coiled geometry in the model and in the electron density distribution, coupled with the kinked structure of rubber and *cis,cis*-farnesol, and the high difference in values of a^* between theoretical and experimental results as well as the third region of high electron density (as indicated under Results) all seem to confirm the determined structure. It appears that the central coiled structure of section B is maintained, with relative flexibility in the flanking arms. The validity of the molecular mechanics method is given by the close agreement of the molecular mechanics derived conformation and crystal structure of squalene (Ernst & Fuhrhop, 1979). The kink in *cis,cis*-farnesol that is responsible for the coiled nature of section B of dolichol is similar to that found in crystalline rubber, a naturally occurring long polymer of *cis*-isoprene (Bunn, 1942). In the original determination of rubber's crystal structure some 40 years ago, rubber was noted to have unique mechanical properties that were similar to those of animal tissue, and it was suggested that there may be a reason for the similarity. It was noted that the methylene group adjacent to double bonds cannot exist in the plane of the isoprene unit, resulting in a coiled structure. The source of the orienting tendency was purported to be intermolecular van der Waals forces. Through use of molecular mechanics, we can demonstrate such kinking as an isolated molecule of *cis,cis*-farnesol, suggesting that the source of this orientation is intramolecular as opposed to intermolecular van der Waals forces. We suggest that the cause for the difference in the kink angle observed in the crystal structure of rubber and in our computer-assisted conformational analysis can be explained by the fact that rubber is crystallized by stretching under great force, and the crystal structure of rubber can be visualized as a stretched-out version of the coiled section B of dolichol-19. Also, rubber is of much greater chain length than dolichol-19.

We feel that the close agreement between the SAXS data derived from the energy-minimized conformation and the actual experimental SAXS data, coupled with the ability of our version of MM2 to predict the crystal structure of squalene, demonstrates MM2's ability to accurately predict the lowest energy conformations of isoprenoids. It should be stressed, however, that MM2 execution may result in generation of a conformation that exists in a local energy minimum, due to the $3N$-dimensional complexity of the potential function

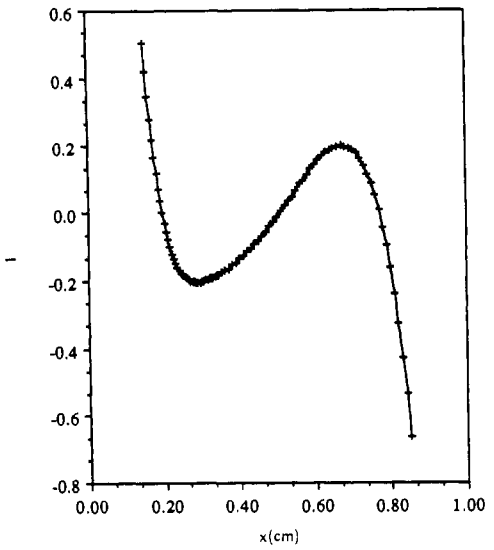

FIGURE 14: Ordering effect of dolichol on oleyl alcohol.

(where N is the total number of atoms plus the lone pair electrons in the molecule in question). While this may imply that our determined conformation of dolichol-19 might not be the global energy minimum, our conformation would be of biological relevance even if it were not the lowest energy form; that is, local minima at higher energy than the global minimum may represent important transitory conformations that exist in the membrane involved in biological processes.

SAXS is more desirable over X-ray diffraction for the determination of conformation in solution as opposed to the solid-state conformation of a molecule. X-ray diffraction, however, will give much better resolution. Due to dolichol's low melting point, −10 °C (Dunphy et al., 1967), X-ray crystallography studies on dolichol have not yet been achieved. It may be possible to form a crystalline derivative by reaction at the hydroxyl group, but this may result in a change in the conformation of the isoprene backbone. Our recent studies (Murgolo et al., 1987) on the extended conformation of dolichol in a penetrating solvent demonstrated the ability of SAXS to study the solution conformation of such a small molecule. SAXS cannot be employed to study dolichol in lipid bilayers, as the strong scattering due to the ordering of the bilayer will greatly mask the scattering due to dolichol (Valtersson et al., 1985). Attempts to use the membrane-mimetic solvent oleyl alcohol have led to similar problems in our laboratory (see Figure 14). For this reason, we chose to employ the relatively impenetrating and unorderable solvent isopentyl alcohol to study the solution conformation of dolichol in that solvent. The concentration of dolichol employed in this scattering experiment was 20 mg/mL, above the previously determined critical micellar concentration (see Figure 13). Since this concentration (20 mg/mL) of dolichol is the minimum concentration of solution for our SAXS, scattering experiments could not be employed to study the solution conformation of dolichol in membrane-mimetic solvents such as oleyl alcohol. However, the similar viscosity behavior (both having negative intrinsic viscosity) of dolichol in isopentyl alcohol and in oleyl alcohol below the critical micellar concentration suggests that solutions of dolichol in isopentyl alcohol are similar in solution fluidity to dilute solutions of dolichol in membrane-mimetic solvents such as oleyl alcohol. Thus, the solution conformation of dolichol in isopentyl alcohol should provide an adequate description of the membrane conformation of dolichol. The quantitative measurement of the effect of dolichol upon solution viscosity of isopentyl alcohol and oleyl alcohol (below the critical micellar concentration) is the first true quantitative measure of the effect of dolichol upon solution fluidity of membrane-mimetic solvents (fluidity is here defined in the dynamic sense as reciprocal viscosity). The solution behavior of this conformation of dolichol suggests that dolichol plays a membrane-fluidizing role in low concentration and gives quantitative measure of the magnitude of dolichol's fluidizing effect.

The importance of the electron density function as it is related to structure, and its determination by X-ray methods, has recently been presented (Hauptman, 1986). Unfortunately, we can only compare conformations in different solvents for the distribution of a theoretical sphere; the distribution functions of cylinders can only be approximated in the case where length is much greater than diameter (Fedorova, 1977). The ability of the SAXS method to study the conformation of molecules as small as dolichol has been presented (Murgolo et al., 1987). The determination of the solution conformation of this relatively compact conformer of dolichol in the relatively large solvent isopentyl alcohol represents an application of the SAXS method in its extreme limit, as we found that it was not possible to obtain scattering above the noise level of the solvent until dolichol concentrations exceed 20 mg/mL. This application of the SAXS method to perhaps one of the smallest molecules other than Orange II (Kratky, 1967) ever analyzed by SAXS coupled with the computer-assisted conformational analysis of the largest molecule attempted with MM2 demonstrated the uniqueness of our experimental approach.

^{31}P NMR evidence has been presented suggesting that both ends of esterified polyisoprenols observe environments deep within the bilayer, with the assertion that esterified polyisoprenols do not adopt the conventional head group at interface orientation (de Ropp & Troy, 1985). We contend that although esterified dolichols may adopt an unconventional orientation, the free alcohol and its phosphorylated derivatives should be expected to adopt a head group at interface orientation, as this would easily allow total membrane inclusion of our current model. In the case of dolichol phosphate, a recent detailed study of its effects on bilayer fluidity has suggested it adoptability to an orientation in which the phosphate group is oriented to the aqueous interface and that its induction of H_{II} phase and its bilayer destabilization in its phosphorylated form may facilitate sugar translocation (van Duijin et al., 1986). Additional support for this hypothesis is provided by noting the luminal and cytoplasmic orientation of enzymes involved in glycosylation of dolichyl phosphate and in sugar transfer. A recent review on the subject suggested that endogenous glycosylated proteins are luminally oriented and polyisoprenol transferase is cytoplasmically oriented, suggesting transbilayer movement of dolichyl phosphoryl sugars (Krag, 1985). Transmembrane topology studies employing enzyme latency of polyisoprenol phosphate phosphatase in rat liver demonstrate that the enzyme is cytoplasmically oriented (Keller et al., 1986). If our determined conformation of dolichol is correct, then we will have achieved conformational characterization of dolichol with regard to its possible membrane function. From our newly determined structure, we hope the mechanism of sugar translocation in the glycosylation of proteins in the rough endoplasmic reticulum will become more evident. Previously, an exact understanding of this mechanism has been prevented by ignorance of the biomembrane conformation of dolichyl phosphate. The biological activity of dolichol and its derivatives undoubtedly is intimately related to its conformation. Dolichyl phosphate must be able to intercalate within subcellular membranes to function in protein

glycosylation and must somehow transport polar sugars from the cytosol to the lumen of the rough endoplasmic reticulum. We feel the conformation of dolichol presented here is an adequate representation of the reticulum membrane conformation of dolichol phosphate, as the conformation of dolichol is largely dependent upon the integrity and preservation of the coil of the central region. Our model possesses several desirable features. It is compact enough to exist entirely within the membrane bilayer, without the unfavorable hydrophobic–hydrophillic interactions associated with a fully extended conformation or with a model in which both ends of the molecule are thought to exist deep within the bilayer. Since previous experiments demonstrate that dolichol and its derivatives have an effect on membrane fluidity, the presence of dolichol-induced local hexagonal phase disruption of the rough endoplasmic reticulum bilayer coupled with the determined "corkscrew-like" conformation would present a plausible mechanism for the membrane transport of sugars in N-linked protein glycosylation.

The membrane-destabilizing effects of dolichol and its derivatives may also implicate dolichol in fusion processes in secretory cells and in transport in organelles, especially given the relatively high presence of dolichol in lysosomes (Wong et al., 1982). In addition to an understanding of the mechanism of sugar transport in N-linked glycosylation, other benefits might be gained in the field of dolichol biochemistry now that we have realized the conformation of dolichol. The mechanisms of action of other dolichol-related enzymes could be better understood. In addition, an understanding of the effect of dolichol and its derivatives on membrane fluidity can now be viewed in light of the unique conformation of dolichol presented above.

Registry No. Dolichol-19, 42436-66-8; squalene, 111-02-4; *trans,trans*-farnesol, 106-28-5; *cis,cis*-farnesol, 16106-95-9; dolichol, 11029-02-0; oleyl alcohol, 143-28-2; isopentyl alcohol, 123-51-3.

References

Allinger, N. L. (1977) *J. Am. Chem. Soc. 99*, 8127–8134.

Allinger, N. L., & Chung, D. Y. (1976) *J. Am. Chem. Soc. 98*, 6798–6803.

Applegate, K. R., & Glomset, J. A. (1986) *J. Lipid Res. 27*, 658–680.

Bunn, C. W. (1942) *Proc. R. Soc. London, A 180*, 40–99.

Burgos, J., Hemming, F. W., Pennock, J. F., & Morton, R. A. (1963) *Biochem. J. 88*, 470–482.

Burkert, U. (1979) *Tetrahedron 35*, 209–212.

Burkert, U., & Allinger, N. L. (1982) *Molecular Mechanics*, ACS Monograph 177, American Chemical Society, Washington, DC.

de Ropp, J. S., & Troy, F. A. (1985) *J. Biol. Chem. 260*, 15669–15674.

Dunphy, P. J., Kerr, J. D., Pennock, J. F., Whittle, K. J., & Feeney, J. (1967) *Biochim. Biophys. Acta 136*, 136–147.

Ernst, J., & Fuhrhop, J. H. (1979) *Liebigs Ann. Chem.*, 1635–1642.

Fedorova, I. S. (1977) *J. Colloid Interface Sci. 59*, 98–105.

Glatter, O. (1977) *J. Appl. Crystallogr. 10*, 415–421.

Hauptman, H. (1986) *Science (Washington, D.C.) 233*, 178–183.

Keller, R. K. (1986) *J. Biol. Chem. 261*, 12053–12059.

Kennan, R. W., Fischer, J. B., & Kruczek, M. E. (1977) *Arch. Biochem. Biophys. 179*, 634–642.

Krag, S. S. (1985) *Curr. Top. Membr. Transp. 24*, 181–249.

Kratky, O. (1967) *Small Angle X-ray Scattering* (Brumberger, H. Ed.) pp 99–105, Gordon & Breach, New York.

Kratky, O. (1983) *Nova Acta Leopold. NF55, No. 256.*

Murgolo, N. J., & Wong, T. K. (1986) *Fed. Proc., Fed. Am. Soc. Exp. Biol. 45*, 1669.

Murgolo, N. J., Patel, A., Stivala, S. S., & Wong, T. K. (1987) *Biopolymers* (submitted for publication).

Struck, D. K., & Lennarz, W. J. (1980) *The Biochemistry of Glycoproteins and Proteoglycan*, Plenum, New York.

Valtersson, C., van Duijin, G., Verkleij, A. J., Chojinacki, T., de Kruijff, B., & Dallner, G. (1985) *J. Biol. Chem. 260*, 2742–2751.

van Duijn, G., Valtersson, C., Chojnacki, T., Verkleij, A. J., Dallner, G., & deKruijff, B. (1986) *Biochim. Biophys. Acta 861*, 211–213.

Weiner, S. J., Kollman, P. A., Case, D. A., Singh, U. C., Ghio, C., Alagona, G., Profeta, S., Jr., & Weiner, P. (1984) *J. Am. Chem. Soc. 106*, 765–784.

White, D. N. J., & Bovill, M. J. (1977) *J. Chem. Soc., Perkin Trans. 2*, 1610–1623.

Wong, T. K., Decker, G. L., & Lennarz, W. J. (1982) *J. Biol. Chem. 257*, 6614–6618.